Extreme Multi-zone (TEMZ) Model for Multi-waveband Variability of Blazars

Alan P. Marscher (Institute for Astrophysical Research, Boston University; marscher@bu.edu)

SUMMARY

The author is developing a model in which much of the optical and high-energy radiation in a blazar is emitted near the 43 GHz core of the jet as seen in VLBA images, parsecs from the central engine. For observational evidence supporting this scenario, see Figs. 2 & 3 and talk by Svetlana Jorstad. The main physical features are a turbulent ambient jet plasma that passes through a conical standing shock wave ("recollimation shock") in the jet. The model allows for short time-scales of optical and gamma-ray variability by restricting the highest-energy electrons radiating at these frequencies to a small fraction of the turbulent cells, perhaps those with a particular orientation of the magnetic field relative to the shock front. Because of this, as well as radiative energy losses as the plasma advects beyond the shock front, the volume filling factor at high frequencies is relatively low, while that of the electrons radiating below about 10 THz is near unity. Such a model is consistent with the following observational trends: (1) red-noise power spectra of flux variations in blazars, (2) shorter time-scales of variability of flux and polarization at higher frequencies, (3) mean polarization levels as well as fractional deviations from the mean that are higher at optical than at lower frequencies, (4) apparent rotations in polarization position angle that are really just random walks of the projected magnetic field direction, (5) breaks in the synchrotron spectrum by more than the radiative loss value of 0.5, and (6) flares that are often sharply peaked or contain multiple peaks, both of which are not not reproduced by single- or few-zoned models. The dependence of items 2-4 on frequency is directly related to the change in spectral index beyond the break, according to the model.

The model includes synchrotron radiation, inverse Compton scattering (IC) of seed photons from hot dust, as found in 4C 21.35 and CTA102 by Malmrose et al. (2011, ApJ, **732**, 116), and IC of synchrotron + SSC radiation from relatively slowly moving plasma in a Mach disk at the vertex of the conical shock. This is the dominant SSC emission, since the seed photons are Doppler boosted in the frame of the turbulent cells. The combined effects of co-spatiality of the emission regions at different wavebands, non-uniform electron energy distribution, different magnetic field orientations for different turbulent cells, and light-travel delays, cause **correlations of variations at pairs of wavebands but with time lags and often a lack of one-to-one correspondence of flares. This is similar to the observed behavior of blazars.** The discrete gamma-ray/optical correlation function is similar to that observed in blazars, with zero mean lag but considerable spread about this value.

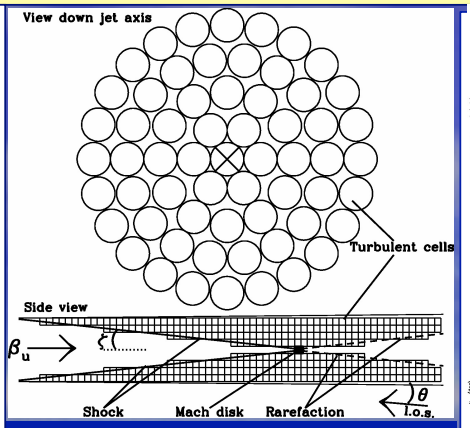

Fig. 1. Turbulent Extreme Multi-zone (TEMZ) Model

The geometry of the model is shown in Fig. 1.The source consists of many cylindrical turbulent cells. The central cell may be a Mach disk (shock oriented transverse to the jet axis, called a "working surface" when it is at the end of a jet) where flow is strongly compressed but relatively slow (<*c*/3). Plasma in other cells see Mach disk emission to be highly blueshifted and therefore amplified. Typical simulation: between 61 and 271 columns of cells across the jet cross-section plus cells along each column downstream of shock until rarefaction is reached ➔ hundreds or thousands of emission zones!

Electrons are energized as a cell crosses the conical shock or Mach disk. Maximum electron energy achieved varies with different cells. For light curves shown here, E_{max} is determined randomly from a power-law probability distribution such that higher values of E_{max} are rarer than lower values. The volume filling factor is therefore smaller, and thus the variability is more pronounced, at higher frequencies. Each 10^{th} cell in a column has a random direction of the magnetic field *B*, and both *B* and relativistic electron density are varied with time according to the observed power spectral density.

PHYSICAL CONSIDERATIONS

The synchrotron flux density of a cell depends on (among other factors):
(1) The volume filling factor of electrons with energies high enough to radiate at the frequency of observation
(2) The spectral index α, determined by the slope of the electron energy distribution
(3) The normalization factor N_0 of the electron energy distribution
(4) The strength and angle of the magnetic field relative to the line of sight (corrected for relativistic aberration) through the factor $(B \sin \psi)^{(1+\alpha)}$

The synchrotron self-Compton/Mach disk X-ray or γ-ray flux density depends on:
(1) The volume filling factor of electrons with energies high enough to scatter the highest-frequency synchrotron photons to the observed photon energy
(2) The slope of the electron energy distribution
(3) The square of the normalization factor N_0 of the electron energy distribution
(4) The strength of the magnetic field through the factor $B^{(1+\alpha)}$
(5) The angle ψ of the magnetic field relative to the line between the cell emitting the synchrotron radiation and the cell doing the inverse Compton scattering (corrected for relativistic aberration) through the factor $(\sin \psi)^{(1+\alpha)}$

The inverse Compton X-ray or γ-ray flux density depends on:
(1) The volume filling factor of electrons with energies high enough to scatter the highest-frequency seed photons to the observed photon energy
(2) The slope of the electron energy distribution
(3) The normalization factor N_0 of the electron energy distribution
(4) The energy density of seed photons, which is constant for photons emitted by a dust torus and nearly constant if from the broad emission-line region, but highly variable if from a relatively slow region inside the jet, such as a Mach disk

Since some of these factors are different for the 3 processes, there will not be a one-to-one correspondence between light curves at two widely separated frequencies despite the electron energies being ~ the same for optical and gamma-ray emission. Even for relatively closely spaced frequencies (e.g., optical and near-IR), differences in volume filling factor as a function of maximum electron energy will weaken the correlations of the light curves and polarization vs. time.

At very high photon energies, "orphan flares" are possible if the magnetic field of the cell that contains the highest energy electrons points directly along the line of sight. In this case, no synchrotron flare would be seen even during a major γ-ray flare.

Inverse Compton flares usually have lower amplitudes relative to the synchrotron variations unless the seed photon density is also variable, as in SSC emission. A Mach disk at the end of a conical recollimation shock can provide such a variable source of seed photons that is well beamed in the frame of the plasma passing through the recollimation shock but not in the observer's frame, since the flow speed of the plasma beyond the Mach disk is only mildly relativistic. Temporarily bright regions in a relatively slow sheath of the jet could produce a similar effect.

The code allows each cell to have a randomly oriented turbulent velocity relative to the general jet flow. This, along with the different maximum electron energy and magnetic field direction in the different cells, as well as the small volume of each cell, allows for very fast variability at optical and γ-ray frequencies (see Narayan & Piran 2012,,*MNRAS*, 420, 604).

As can be seen by comparing the results of a simulation (Fig. 4) with actual data (Figs. 2 & 3), the results look quite promising. After the remaining desired features (see list to right) are added to the code, we will run it over a range of input parameters to determine the physical conditions under which various observational features can be reproduced.

Acknowledgements: This research has been supported in part by NASA through Fermi grants NNX08AV65G, NNX10AO59G, and NNX11AQ03 in the past, and is currently supported by Fermi grant NNX12AO79G, for which the author is grateful.

Observational Motivation: 3C 454.3

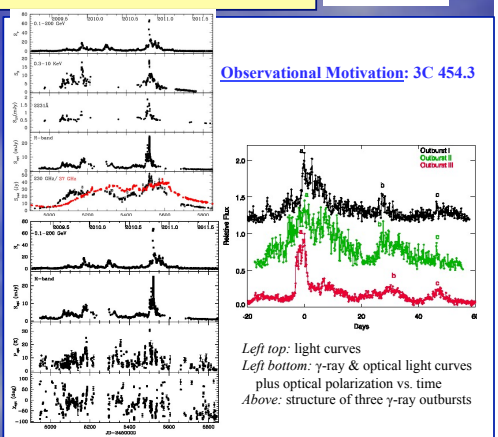

Left top: light curves
Left bottom: γ-ray & optical light curves plus optical polarization vs. time
Above: structure of three γ-ray outbursts

Fig. 2: Flux and polarization curves of 3C 454.3 from Jorstad et al. (2013, in prep). Much of the data is also published in Wehrle et al. (2012, ApJ, **758**, 72).

Observational Motivation: BL Lac

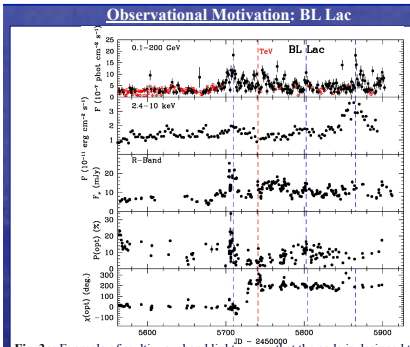

Fig. 3a: Example of multi-waveband light curves that the code is designed to imitate. Note the differences in the light curves among the wavebands as well as the fluctuations in polarization. Data from Marscher et al. (in preparation)

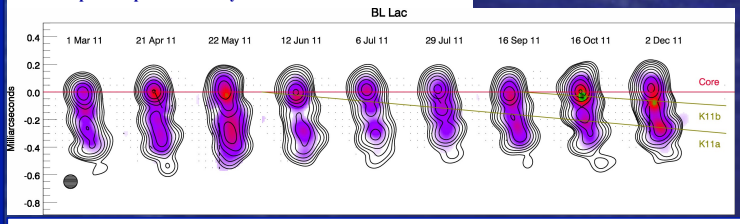

Fig. 3b: Sequence of 43 GHz VLBA images of BL Lac in 2011. Contours: total intensity; color: linear polarization. Position of "core" and trajectories of two new superluminal knots are indicated. The knots passed through the core on JD-2450000 = 5712±15 and 5845±10. Both γ-ray outbursts occurred as the knots passed through stationary emission features within 3 mas of the core.

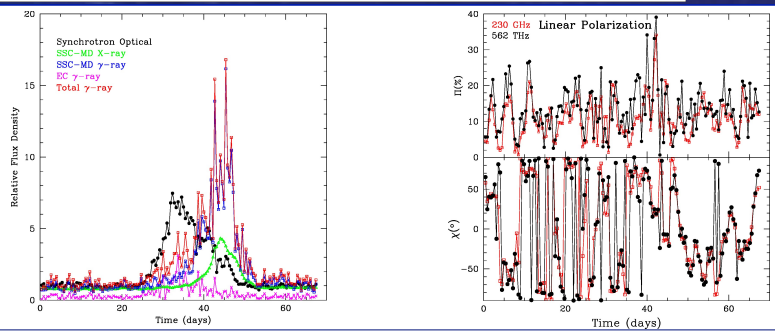

Fig. 4: *Left:* Sample light curves from synchrotron radiation + inverse Compton scattering of seed photons emitted by a dust torus or Mach disk by electrons in the turbulent cells, from a TEMZ simulation with input parameters similar to those inferred observationally for 3C 454.3. Ourburst was artificially introduced with an exponential rise and decay of a higher energy density of relativistic electrons. Note the various ratios of high-energy to optical flux. Outburst is induced by increase in electron energy density with exponential rise and fall over 20 days.
Right: Linear polarization vs. time at optical and 1 mm wavelengths from the same simulation. Note that the degree of polarization is typically ~10% but fluctuates on short time-scales. The position angle of polarization χ tends to lie transverse to the jet (90° in the figure), but also undergoes rotations (in both directions) during the outburst. Both characteristics are observed in 3C 454.3.

Work to be done to add features to code (with graduate student Michael Valdez:

- **Allow slope of energy distribution of relativistic electrons to depend on direction of magnetic field relative to shock (see Summerlin & Baring 2012, *ApJ*, 745, 63)**
- **Refine synchrotron self-absorption calculation to prodice more accurate lower frequency results**
- **Simulate magnetic turbulence better by relating magnetic field vectors of adjacent cells in transverse direction**
- **Add cell-to-cell SSC (will require moving to a supercomputer**
- **Add pair-production opacity**